PHYSICAL REVIEW E **74**, 035302(R) (2006)

Periodic sedimentation in a Stokesian fluid

Sunghwan Jung, S. E. Spagnolie, K. Parikh, M. Shelley,* and A-K. Tornberg
Applied Mathematics Laboratory, Courant Institute of Mathematical Sciences, New York University, 251 Mercer Street, New York, New York 10012, USA

(Received 4 May 2006; published 8 September 2006)

We study the sedimentation of two identical but nonspherical particles sedimenting in a Stokesian fluid. Experiments and numerical simulations reveal periodic orbits wherein the bodies mutually induce an in-phase rotational motion accompanied by periodic modulations of sedimentation speed and separation distance. We term these "tumbling orbits" and find that they appear over a broad range of body shapes.

DOI: 10.1103/PhysRevE.74.035302 PACS number(s): 47.57.ef, 47.63.mf, 47.54.De, 47.27.ek

The dynamics of bodies settling through a Stokesian fluid has a long and important history in fluid dynamics, and remains relevant to natural and industrial phenomena of contemporary interest [1]. In 1851, Stokes determined the settling speed U of a solid sphere of radius a and density $\bar{\rho}$, showing that $U=\frac{2}{9}\frac{a^2 g}{\mu}(\bar{\rho}-\rho)$, where μ and ρ are the fluid viscosity and density, respectively [2]. Stimson and Jeffery [3] considered two sedimenting spheres of equal density and radius, with one placed above the other, and showed that the settling speed is increased by their interaction through the fluid. Exact series solutions for two identical spheres arbitrarily situated have since been derived [4].

The case of nonspherical bodies is much less studied analytically, and few exact solutions exist. Oberbeck [5] and Jeffery [6] determined the settling dynamics of a single ellipsoid, indicating that a sedimenting ellipsoid of revolution has no tendency to change its orientation, and that its speed (an increasing function of ellipticity) increases monotically as its major axis changes from the horizontal to the vertical. Problems involving many bodies are less understood, and are almost the exclusive domain of experiment, approximation, or large-scale simulation. For example, it has been observed numerically that three or more settling particles (treated approximately) in a viscous fluid can exhibit very complicated, if not chaotic, dynamics [7] (see also the experiments in Ref. [8]). The interaction of many slender bodies has been studied in some detail [9–12].

Here we study, by experiment and numerical simulation, the sedimentation dynamics of two identical bodies of various nonspherical shapes. Given appropriate initial configurations, we find that each body can induce a mutual rotation upon the other that leads to visually striking periodic dynamics that we term "tumbling orbits." In these orbits, each body simultaneously rotates and separates from the other in a mirror-symmetric fashion (the spreading and slowing resembles visually the dynamics of an opening parachute). After achieving their greatest separation, the bodies continue to rotate and accelerate as they fall towards each other; the process then begins anew. These orbits appear to be stable, and are reproduced over a wide range of body types including disks, rods, hemispheres, and cubes. The stability of tumbling orbits with three or more bodies and the effects of different initial placements are studied numerically. Our results are consistent with theoretical treatments for ellipsoids [13–15], which have predicted the existence of such orbits when the bodies are well separated.

Experiments. The experimental setup is illustrated in Fig. 1. A tall transparent container is filled with silicone oil. Two different oils are used, each with large viscosity ($\nu=10^3$ and 10^4 cS, $\rho=0.98$ g/cm^3). These oils behave as Newtonian fluids in the regime of interest here. At the top free surface, we introduce bodies of various shapes and sizes. The bodies are made of a plastic slightly heavier than the fluids ($\bar{\rho}=1.12$ g/cm^3). We focus primarily on the dynamics of disk- and rod-shaped bodies. The rods are of fixed diameter ($d=0.32$ cm) and of various lengths ($L=0.5$–2 cm); the disks are of fixed thickness ($d=0.16$ cm) and of various diameters ($L=0.5$–2.6 cm). The body pairs are constructed to have the same volume by cutting and sanding to precise dimensions. The body positions, orientations, and velocities are measured from a 30 frame per second video stream. Other experiments, not reported in detail here, studied the dynamics of pairs of spheres, hemispheres, and cubes.

Other sedimentation experiments have been initiated using various body-release mechanisms [8,16,17]. For our purposes here, we found it difficult to place the bodies in the precise desired initial configurations, but we chanced upon a method of release. The plastic material of the bodies is not wetted by the oil, allowing them to "float" on the supporting

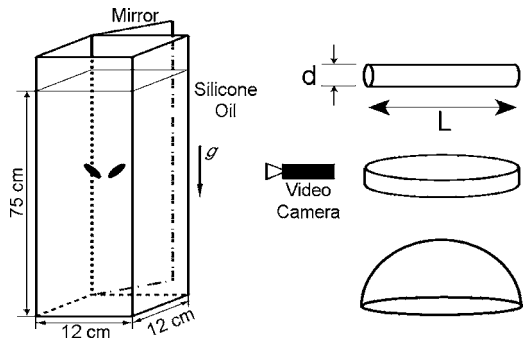

FIG. 1. Schematic of the experimental setup. Silicone oils fill the transparent vessel. By pushing the bodies into the fluid with a wire mesh, the initial condition is well controlled. A mirror is placed at a 45° angle for the side view. Both front and side views are imaged simultaneously through a video camera 1.5 m away.

*Electronic address: shelley@cims.nyu.edu

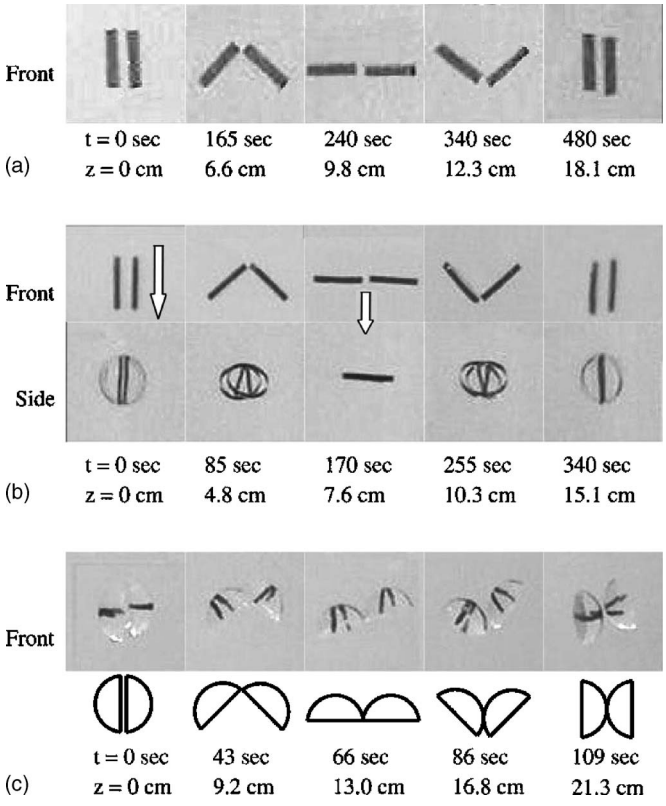

FIG. 2. Snapshots of tumbling orbits for pairs of bodies of various shapes: (a) Rods ($L=1.3$ cm), (b) disks ($L=1.3$ cm), (c) hemispheres ($L=1.3$ cm). The last row of hemispheres reproduces the previous row in schematic form. We observe that the right (left) body rotates in a counterclockwise (clockwise) direction. After rotating 180° (rods and disks) or 360° (hemispheres), they return to their initial configuration. Rod and disk pairs fall nearly twice as fast when aligned to gravity than when orthogonal (illustrated by arrows).

menisci if placed carefully on the top free-surface. This allows us to lay out an initial, though restricted, set of precise body configurations there. The bodies are then pushed vertically into the fluid using a flat wire mesh. After the release, terminal dynamics are typically approached within a sedimentation distance of approximately $5L$. During this stage there is a decrease in the separation distance (the causes of which will be discussed below), and our experimental results do not depend significantly upon the initial separation distance for this reason. Due to the small difference between body and fluid densities, and the high viscosity of the fluids, the Reynolds numbers ($\mathrm{Re}=\rho UL/\mu$) in the experiments are small, ranging from 10^{-4} to 10^{-1}. Likewise, the Froude numbers [the ratio of inertial force to gravitational force $\mathrm{Fr}=\rho U^2/(\bar{\rho}-\rho)gL$] are small, ranging from 10^{-6} to 10^{-3}.

Experimental results are shown in Fig. 2. Figure 2(a) shows the rotational dynamics of a pair of identical rods over an orbit well separated from the top free-surface. At the beginning of this period, the two rods are aligned and descending at the maximal velocity of the orbit. Roughly speaking, there is a mutually induced rotation as each body descends in the shear field of the other. As the rods rotate out of the vertical their descent velocities decrease, as suggested by the

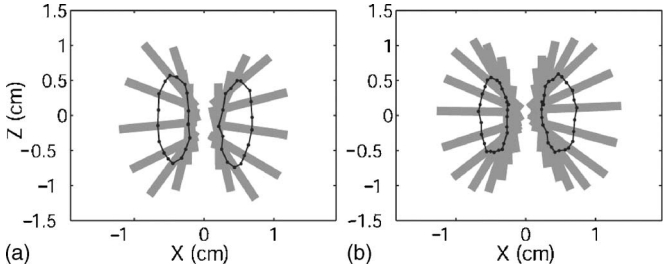

FIG. 3. Two falling disks (a) and rods (b), each held in a uniformly moving frame. Disks are falling at approximately 0.045 cm/s and rods at 0.035 cm/s. Body locations are shown in gray, and are measured every 20 s for disks and rods. Centers of mass are indicated by points and are measured twice as frequently.

single-body results for ellipsoids (see Refs. [5,6,13]). Figure 2(b) shows the qualitatively similar dynamics for a pair of disks. We observe that two bodies sediment on average faster than the maximum possible velocity of a single body (~1.5 times; see Fig. 4). Finally, Fig. 2(c) shows a half period of the tumbling orbit for two hemispheres.

A central feature of the tumbling orbits is the oscillation of each body's center of mass, shown in Fig. 3 for both disks and rods. Here the motion is captured in a frame moving with the mean velocity, and in this frame the orbit is in each case approximately a 2:1 ellipse. The vertical extent of this ellipse shows the departures from constant settling velocity induced by the rotation. The horizontal distance shows to what extent the two bodies alternately push each other away, and pull each other together. That this orbit is closed when in this constant velocity frame is indicative of its stability.

Figure 4 shows the average descent velocity as L is varied. Given the low Reynolds numbers, scaling velocity by viscosity should remove the viscosity dependency in the data; hence, the separation of the data points for the largest body size is likely due to finite Reynolds number effects. For both disks and rods we find a velocity mostly increasing with length, though for rods this increase is much weaker. For disks the increase is linear at smaller lengths, with departures that we attribute to interaction with the container walls (see also Ref. [18]). The velocity scaling and dependencies can be understood through very simple considerations. By balancing drag forces and gravitational forces one finds the estimate $U\sim(g|\bar{\rho}-\rho|d^{3-n})L^{n-1}/\mu$, where $n=2$ for disks and $n=1$ for rods. The period is estimated as $T\sim L/U\sim(d^{n-3}/g|\bar{\rho}-\rho|)\mu L^{2-n}$. This is in rough agreement with the data in Fig. 4.

Simulations. We have been able to reproduce many of our experimental observations in simulations of bodies settling in a Stokesian fluid. The Stokes equations are

$$\nabla\cdot\mathbf{S}=-\nabla p+\mu\Delta\mathbf{u}=\rho g\hat{\mathbf{z}},\quad \nabla\cdot\mathbf{u}=0, \tag{1}$$

where $\mathbf{S}=-p\mathbf{I}+2\mu\mathbf{E}$ is the stress tensor with p the pressure, $\mathbf{u}$ the fluid velocity, and $\mathbf{E}$ the symmetric rate-of-strain tensor. Consider N solid bodies immersed in a fluid, where the kth body has center of mass at $\mathbf{X}^{(k)}(t)$ and surface labeled as B_k, $k=1,\ldots,N$, with external normal $\hat{\mathbf{n}}^{(k)}$. All bodies are taken as geometrically identical, each having density $\bar{\rho}$ and

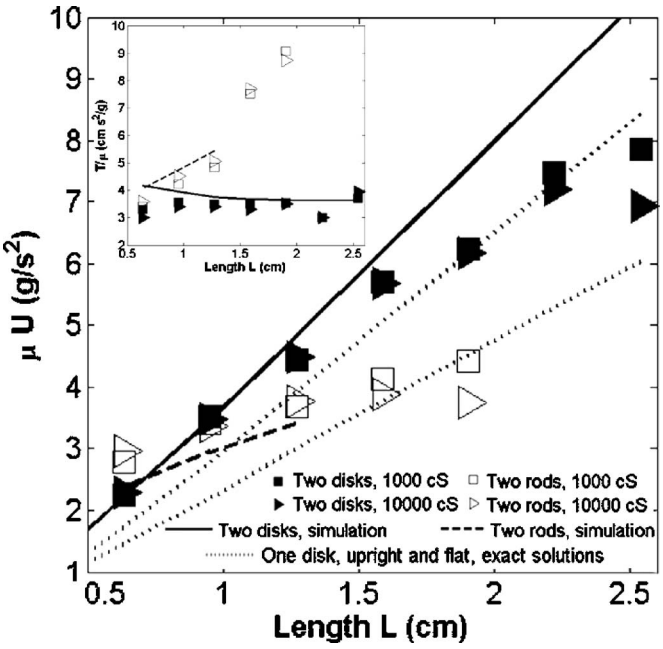

FIG. 4. Experimental and simulational mean velocities and periods as the length L is systematically changed; two disks and two rods, in 1000 cS and 10 000 cS silicone oils. The dotted lines show the exact solutions for a single disk; the solution follows the lower curve if the body's minor axis and gravity are parallel, and the steeper curve if they are orthogonal.

volume V. The no-slip condition is applied at each body surface, and applied forces and torques acting on the kth body must balance the force and torque exerted by the fluid or

$$\int_{B_k} dA_x \mathbf{S}\cdot\hat{\mathbf{n}} = \bar{\rho} g V \hat{\mathbf{z}}, \quad \int_{B_k} dA_x (\mathbf{x}-\mathbf{X}^{(k)})\times\mathbf{S}\cdot\hat{\mathbf{n}} = 0 \quad (2)$$

as gravity exerts no torque. We neglect the presence of the containing walls and surfaces, and consider the fluid as occupying all space.

A number of asymptotic approximation methods have been used to study this class of problems [14,19,20]. We instead solve the Stokes equations exactly, up to discretization errors, using a boundary integral formulation [21]. A representation formula is obtained by placing a Stresslet distribution of unknown vector density $\mathbf{q}$ on the body surfaces [21]:

$$\mathbf{u}(\mathbf{x}) = \sum_k \int_{B_k} dA_{x'} \mathbf{K}(\mathbf{x}'-\mathbf{x})\mathbf{q}(\mathbf{x}') + \frac{1}{8\pi\mu}\sum_k \mathbf{G}(\mathbf{x}-\mathbf{X}^{(k)})\mathbf{F}^{(k)} + \mathbf{G}^c(\mathbf{x}-\mathbf{X}^{(k)})\mathbf{T}^{(k)}, \quad (3)$$

where

$$K_{ij}(\mathbf{x}) = -6(\hat{x}_i\hat{x}_j\hat{x}_k/|\mathbf{x}|^5)\hat{n}_k \quad \text{with} \quad \hat{\mathbf{x}} = \mathbf{x}/|\mathbf{x}|, \quad (4)$$

$$G_{ij}(\mathbf{x}) = (\delta_{ij}+\hat{x}_i\hat{x}_j)/|\mathbf{x}|, \quad G^c_{ij}(\mathbf{x}) = \epsilon_{ijk}\hat{x}_k/|\mathbf{x}|^3. \quad (5)$$

$\mathbf{K}(\mathbf{x})$ is the Stresslet kernel applied to the local normal vector. $\mathbf{G}(\mathbf{x}-\mathbf{X}^{(k)})$ and $\mathbf{G}^c(\mathbf{x}-\mathbf{X}^{(k)})$ are point Stokeslets and Rotlets internal to the kth body, and $\mathbf{F}$ and $\mathbf{T}$ are the external forces and torques on the bodies. With the assumption of rigid body motion $\mathbf{u}^{(k)}=\mathbf{U}^{(k)}+\Omega^{(k)}\times(\mathbf{x}-\mathbf{X}^{(k)})$, this representation generates a (well-conditioned) second-kind integral equation with a unique solution $(\mathbf{q},\mathbf{U},\boldsymbol{\Omega})$ and solves Eqs. (1), (2). Equation (3) is made nondimensional and free of adjustable parameters by scaling $\mathbf{x}\to L\mathbf{x}$, $\mathbf{u}\to U\mathbf{u}$, $\mathbf{q}\to U\mathbf{q}$. Here, $\mathbf{F}^{(k)}=-\hat{\mathbf{z}}$ and $\mathbf{T}^{(k)}=\mathbf{0}$. The dynamics then depend only upon the geometric shapes of the bodies and their initial configurations.

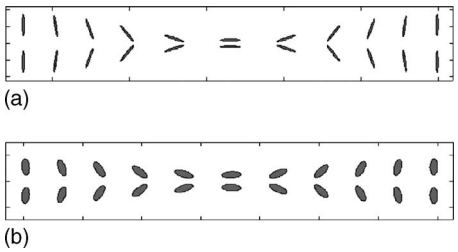

FIG. 5. From simulation, the settling dynamics of two falling, identical bodies; (a) two prolate ellipsoids, aspect ratio 8:1 and (b) two oblate ellipsoids, aspect ratio 1:3.

Note the time reversal symmetry found by $\mathbf{g}\to-\mathbf{g}$, of which the left-right symmetry in Fig. 5 is a consequence. By this symmetry it may also be shown that the distance between two spheres sedimenting one atop the other does not change (this argument may be extended to ellipsoids). Moreover, the symmetry ensures that after each period of a tumbling orbit, there is no change in the separation distance between the two bodies. In conjunction with the fact that body positions are determined by a first order ODE (orbits do not cross in phase space), this shows that all tumbling orbits are truly periodic.

In the numerical simulations, disks and rods are approximated by flat oblate ellipsoids and elongated prolate ellipsoids, respectively. Each body is represented by a surface grid, and applying a Nyström collocation method produces a system of linear equations for the density $\mathbf{q}(\mathbf{x})$ at the grid points, which is then solved iteratively. The (weakly singular) integrals are computed to second order in the surface mesh element size. Body positions and orientations are updated using a second-order Runge-Kutta method. Both convergence tests and comparison with known exact solutions [2–4,6] were used to validate the code.

We have used simulations to explore many aspects of this system. Figure 5 shows numerical simulations of falling pairs of oblate and prolate ellipsoids (i.e., "disks" and "rods"), reproducing the tumbling dynamics observed in experiment. As indicated in Fig. 4, the general trends are recovered by our numerical efforts; possible discrepancies may be attributable to wall effects or to the different body geometries used in experiments and simulations. The one available free parameter with which we are able to match simulations with initial data is the initial separation distance; setting this parameter to $L/8$ gives a reasonable account of the experimental data. There is no numerical data for longer prolate ellipsoids in Fig. 4, as the simulated bodies approach collision with this initial separation distance, rendering the fluid dynamic model incomplete and our simulations inaccurate.

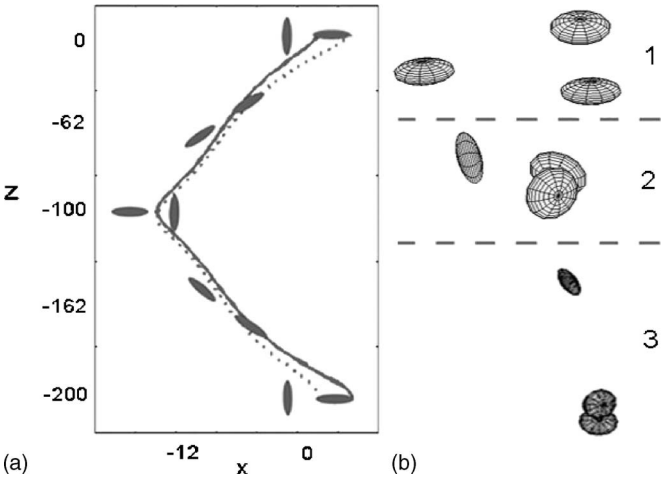

FIG. 6. (a) Different initial orientations of two disks show remarkable periodic orbits; the dotted and solid lines follow one body's edges. The vertical scale has been condensed to show an entire half-period in one plot (the bodies have each rotated 180° in this image). (b) Three bodies reveal an unstable periodic orbit; images 1–3 show orientations at different times, suggesting the onset of instability and the eventual dramatic consequences.

We find in simulation that slightly perturbing the initial positions, for example by tilting one body relative to the other, leads to periodic dynamics very close to those already described. Large perturbations, however, can lead to very different periodic dynamics. For example, by starting with one body aligned orthogonally to the other, we have observed the complicated and beautiful dynamics shown in Fig. 6(a). This we hope to observe experimentally with a new release mechanism.

We have also used simulations to understand a decrease in separation distance seen in the early stages of the experiments. To do so we studied a four body problem with mirror-image symmetry about a free-surface: two bodies are placed just below the surface, and two more bodies are placed symmetrically above and are acted upon by an external force of opposite sign. By symmetry, the velocities normal to the surface produced by both pairs must cancel on the free-surface, and the velocity field created by one pair may be seen to induce attracting velocities on the other set. That the side walls act to slow the sedimenting velocities [18] likely increases the amount of time the bodies spend in this initial stage.

We find numerically that groups of three or more bodies, placed symmetrically, will again achieve tumbling dynamics but we find that if this arrangement is perturbed slightly [as in Fig. 6(b)], the nearly periodic dynamics will disintegrate towards a state with paired bodies descending quickly, and solo laggards left behind. Tumbling orbits of multiple rods and their instability have been observed in numerical studies via slender body theory [22].

In conclusion, we have studied bodies of various shapes interacting while sedimenting in a viscous fluid, and have observed through both experimental and numerical means the existence of tumbling dynamics. We achieved good correlation between the experimental and simulational results, and made predictions about other types of orbits. Future work will focus on the nature of such orbits when nonreversible forces are present, as in non-Newtonian fluid environments.

We thank N. Vandenberghe for helpful discussions and acknowledge support by the DOE (Grant No. DE-FG02-88ER25053) and NSF (Grant No. DMS-0412203).

[1] A. Zeidan, S. Rohani, A. Bassi, and P. Whiting, Rev. Chem. Eng. **19**, 473 (2003).
[2] G. G. Stokes, Trans. Cambridge Philos. Soc. **9**, 8 (1851).
[3] M. Stimson and G. B. Jeffery, Proc. R. Soc. London, Ser. A **111**, 110 (1926).
[4] A. J. Goldman, R. G. Cox, and H. Brenner, Chem. Eng. Sci. **21**, 1151 (1966).
[5] A. Oberbeck, J. Reine Angew. Math. **81**, 62 (1876).
[6] G. B. Jeffery, Proc. R. Soc. London, Ser. A **102**, 161 (1922).
[7] I. M. Janosi, T. Tel, D. E. Wolf, and J. A. C. Gallas, Phys. Rev. E **56**, 2858 (1997).
[8] K. Jayaweera, B. J. Mason, and G. W. Slack, J. Fluid Mech. **20**, 121 (1964).
[9] A. K. Tornberg and M. J. Shelley, J. Comput. Phys. **196**, 8 (2004).
[10] A. K. Tornberg and K. Gustavsson, J. Comput. Phys. **215**, 172 (2006).
[11] J. E. Butler and E. S. G. Shaqfeh, J. Fluid Mech. **468**, 205 (2002).
[12] B. Herzhaft, E. Guazzelli, M. B. Mackaplow, and E. S. G. Shaqfeh, Phys. Rev. Lett. **77**, 290 (1996).
[13] S. Kim, Int. J. Multiphase Flow **12**, 469 (1986).
[14] I. L. Claeys and J. F. Brady, J. Fluid Mech. **251**, 448 (1993).
[15] S. Wakiya, J. Phys. Soc. Jpn. **20**, 1502 (1965).
[16] A. M. D. Amarakoon, R. G. Hussey, B. J. Good, and E. G. Grimsal, Phys. Fluids **25**, 1495 (1982).
[17] G. F. Eveson, E. W. Hall, and S. G. Ward, Br. J. Appl. Phys. **10**, 43 (1959).
[18] A. M. J. Davis, Phys. Fluids A **2**, 301 (1990).
[19] A. Chwang and T. Wu, J. Fluid Mech. **67**, 787 (1975).
[20] R. E. Johnson, J. Fluid Mech. **99**, 411 (1980).
[21] H. Power and G. Miranda, SIAM J. Appl. Math. **47**, 689 (1987).
[22] A. K. Tornberg (private communication).